It is still possible that the formalism will lead to physically absurd results and may therefore be rejected on that account. Since the particle masses are dynamical variables, one might question whether, with interactions present, the particle masses are separately conserved. In the analogous nonrelativistic case, the separate particle energies are not conserved but only the total energy. We shall see that the particle masses are individually conserved if the functional M is of the form of Eq. (18). To be more precise, we shall show that if two particles scatter according to Eqs. (19) and (20) and the interaction term becomes negligible as τ_1 and τ_2 approach $\pm\infty$, then $p_1^2(-\infty)=p_1^2(+\infty)$ and $p_2^2(-\infty)=p_2^2(+\infty)$. To see that this is true, one need only notice that, given the trajectory of particle 2, the trajectory of particle 1 is determined by equations identical in form to the single-particle covariant Hamiltonian equations with

$$M(x_1,p_1)=(p_1^2)^{1/2}+\int I(x_1,p_1,x_2,p_2)d\tau_2. \quad (21)$$

But these equations lead to the conservation of $M(x_1,p_1)$ which, as $\tau\rightarrow\pm\infty$, approaches its free-particle form $M=(p_1^2)^{1/2}$. Of course, in the interaction region, p_1^2 is no longer equal to M_1^2. This fact is not peculiar, being true even for the case of a single particle in an electromagnetic field. One interesting consequence of these equations is that the variable τ_1 is not given by

$$d\tau_1=[(dx_1)^2]^{1/2}$$

except in the asymptotic regions. It is thus not equivalent to the geometrically defined proper time.

PHYSICAL REVIEW VOLUME 167, NUMBER 5 25 MARCH 1968

Generation and Detection of Dynamic Newtonian Gravitational* Fields at 1660 cps

J. A. SINSKY
Department of Physics and Astronomy, University of Maryland, College Park, Maryland
(Received 18 August 1967)

The very-near-zone dynamic Newtonian gravitational fields of an acoustically stressed cylinder are measured as a function of distance and azimuthal angle. The high frequency of 1660 cps is a new regime for gravitational technology, since previously measured gravitational interactions were static, as in the Cavendish experiment, or at tidal cycles per day. Results are in agreement with theory.

INTRODUCTION

APPARATUS responsive to the Riemann tensor was developed[1,2] for the purpose of searching for gravitational radiation. Because it was necessary to calibrate this apparatus in the laboratory, a new local source of dynamic Newtonian gravitational fields was built.[3] The source, or generator, consists of a volume in which large acoustic stresses are maintained by electromagnetic means. In this paper the differential equation of the generator is stated, solved, and from its solution, the gravitational potential function ϕ is obtained. The interaction of ϕ with another larger volume, the gravitational radiation detector, is then considered and the resulting equation of motion of the detector is solved for various spatial configurations with respect to the generator. All calculations are written in the language of Newton. The generator apparatus is then described and the experimental results are given and compared to theoretical predictions.

I. CALCULATION OF THE GRAVITATIONAL POTENTIAL OF THE GENERATOR

The dynamic Newtonian field generator is a 300-lb, 8-in.-diam, 5-ft-long solid aluminum cylinder. It is suspended by wire in a milled groove about its center in a vacuum chamber. In order to induce motion in it with respect to its center of mass, 2-in.-square pads of piezoelectric barium titanate crystals are epoxied to the surface of the bar. These transducers are polarized such that when an alternating electric field is applied to them in a direction normal to the surface that is bonded, they oscillate in a direction parallel to the bar axis. When a large ac voltage is applied to the transducers (2000 V peak-to-peak) at the fundamental longitudinal resonant frequency of the high-Q generator cylinder, high dynamic strains (10^{-4}) are produced in the bar.

The acoustic wave equation for the motion of an elastic bar with damping, in the approximation that each plane cross section of the bar remains plane during

* Supported in part by the U. S. Air Force Office of Scientific Research.
[1] J. Weber, *General Relativity and Gravitational Waves* (Interscience Publishers, Inc., New York, 1961), Chap. 8.
[2] J. Weber, Phys. Rev. Letters **17**, 1228 (1966).
[3] J. Sinsky and J. Weber, Phys. Rev. Letters **18**, 795 (1967).

the motion and that the stress over it is uniform, is

$$\rho\frac{d^2\xi}{dt^2}-Y\frac{d^2\xi}{dz'^2}+r\frac{d\xi}{dt}=0, \tag{1}$$

where ρ=density of the bar, Y=Young's modulus of the bar, r=dissipative constant, ξ=displacement of a point in the bar in the z' direction, z'=coordinate measured parallel to the longitudinal bar axis, and $z'=0$ corresponds to the center of the bar.

The solution of this differential equation for our particular problem is

$$\xi(z',t)=A_1\sin(\pi z'/2l)e^{i\omega t}, \tag{2}$$

where $2l$=the length of the bar, $\omega=2\pi$ times the frequency of oscillation of the bar with respect to its center of mass, A_1=amplitude of the bar oscillations $=(2l/\pi)\epsilon_0$, ϵ_0=strain measured at the center of the bar$=(d\xi/dz')_{z'=0}$. (For most of this experiment, $\epsilon_0=0.5\times10^{-4}$.)

The gravitational potential, ϕ, from the generator is given by the expression

$$\phi(x_\alpha,t)=G\int\frac{\rho(x_\alpha',t')dV'}{D(x_\alpha,x_\alpha')}, \tag{3}$$

where G=constant of gravitation, x_α=field point coordinate, x_α'=source point coordinate, $t'\simeq t$ in the near zone of the generator, and $D(x_\alpha,x_\alpha')$=distance between x_α and x_α'.

This expression is applied to the case of the vibrating cylindrical bar. When the bar is vibrating in its longitudinal mode, its mass remains approximately the same while its volume varies, and, hence, the density of the bar as well as its length boundaries are time-dependent.

$$\phi(x_\alpha,t)=G\int^{\text{time-dependent limits}}\frac{\rho_0[1-\epsilon(x_\alpha',t)+\text{terms of } O(\epsilon^2) \text{ and higher}]\,dV'}{D(x_\alpha,x_\alpha')}, \tag{4}$$

$$\epsilon(z',t)=\left(\frac{\partial\xi(x_\alpha',t)}{\partial x_\alpha'}\right)_{x_\alpha'=z'}=\text{strain in the generator at } x_\alpha'=z' \text{ and at time } t,$$

ρ_0=time-independent density of the generator.

The potential function ϕ for a cylindrically symmetric generator, obtained by expanding (4) and using various Bessel function identities, is, for $z>l$, $r^2=x^2+y^2$, where r=radial distance measured from the z axis of symmetry,

$$\frac{\phi(r,z>l,t)}{G\rho_0}=\int_0^\infty\frac{2\pi\mu}{\alpha k^2}J_1(\mu\alpha k)J_0(\alpha kr)e^{-\alpha kz}[e^{\alpha kl}-e^{-\alpha kl}]dk$$

$$+\int_0^\infty\frac{2\pi\mu k}{1+k^2}J_1(\mu\alpha k)J_0(\alpha kr)A_1e^{i\omega t}[e^{\alpha kl}+e^{-\alpha kl}]e^{-\alpha kz}dk. \tag{5}$$

The first term on the right in Eq. (5) is the gravitational static potential due simply to the mass of the generator. The second term on the right, however, is the dynamic gravitational potential due to the motion of this cylinder with respect to its center of mass. k=a dimensionless dummy variable, μ=radius of the generator=10.16 cm, $l=\frac{1}{2}$ length of the generator=77 cm, and $\alpha=\pi/2l=0.02$ cm^{-1}.

$\phi(r,z>l,t)$ was computed on the IBM 7090 computer at the University of Maryland and the field pattern shown in Fig. 1 was obtained, where the lines are the equipotentials.

II. CALCULATION OF THE STRAIN INDUCED IN THE DETECTOR BECAUSE OF ITS POSITION IN THE DYNAMIC FIELD OF THE GENERATOR

The detector of the dynamic Newtonian field is a $1\frac{1}{2}$-ton aluminum cylinder.[1,2] In order to describe the motion of the detector in the dynamic field of the generator, we must write down its equation of motion with the gravitational force as the driving term. Figure 2 shows the generator and detector coordinate systems. In order to facilitate the calculation of this problem in cylindrical coordinates, the longitudinal axes of the generator and the detector were always parallel. Here, in Sec. II, the unprimed coordinates refer to the generator system and the primed coordinates to the detector system. The origin of each coordinate system is coincident with the geometric center of its corresponding bar. The center-to-center distance between the generator and the detector is $\bar{d}$ and the transverse displacement of the bar axes is $R=\bar{d}\sin\theta$.

The differential equation for the motion of the detector along its z' axis is

$$\left(\rho_D\frac{d^2}{dt^2}-Y_D\frac{d^2}{dz'^2}+r_D\frac{d}{dt}\right)\xi'(x',y',z',t')$$

$$=-\rho_D\frac{d}{dz'}\phi'(x',y',z',t'), \tag{6}$$

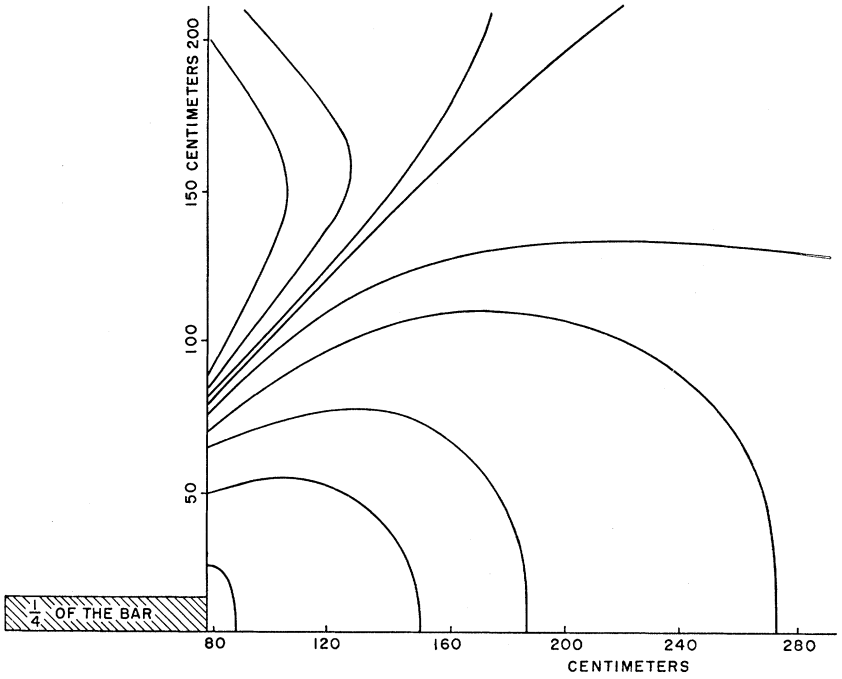

FIG. 1. Lines of constant ϕ dynamic in one quadrant of bar pattern. (By symmetry, the pattern is reproducible in each quadrant.)

where the subscript D refers to detector parameters. In order to find $\phi'(x',y',z',t')$ we must find $\phi(x,y,z,t)$ and substitute as follows:

$$x=\bar{d}\sin\theta+x',$$
$$z=\bar{d}\cos\theta+z',$$
$$y=y'.$$

The total gravitational potential of the excited generator is written as the sum of a static and dynamic potential, the latter having the coefficient $e^{i\omega t}$. This can be expressed in the detector coordinate system by the expression

$$\phi'(x',y',z',t')=\phi_{\mathrm{St}}'(x',y',z')+\phi_{\mathrm{Dyn}}'(x',y',z')e^{i\omega t}. \quad (7)$$

Similarly, we can write for the displacement ξ' in the detector

$$\xi'(x',y',z',t')=\xi_{\mathrm{St}}'(x',y',z')+\xi_{\mathrm{Dyn}}'(x',y',z')e^{i\omega_D t'},$$

where ξ_{St}' is the displacement due to the static component of the field and ξ_{Dyn}' is the displacement due to the dynamic component of the field. ξ_{St}' is merely the total shift of one bar relative to a fixed point in space due to the static field of the other bar. This would occur regardless of the motion of either bar with respect to its center of mass. Since we are interested only in the motion of the detector with respect to its center of mass, we will only investigate the dynamic equation.

Assume that the force on a $z'=$const plane of the detector resulting from the dynamic gravitational field of the generator is the average force on that plane.

$$\text{Average force}=\frac{1}{\text{area of plane}}\int_0^{\text{radius}}\frac{d\phi'(z',r')}{dz'}dA', \quad (8)$$

where $(r')^2=(x')^2+(y')^2$. Calculating the displacement in the detector from the differential equation describing its motion, we obtain for the general case of detector and generator parallel, but not necessarily coaxial,

$$|\xi_{\mathrm{Dyn}}'(z',R)|=\int_0^\infty\frac{B(k)4LQ_D\alpha k}{\pi^2(\alpha^2k^2+\pi^2/4L^2)}\times(e^{\alpha kL}+e^{-\alpha kL})\sin\left(\frac{\pi z'}{2L}\right)dk, \quad (9)$$

$$B(k)=-\frac{2\rho_D}{Y_D}\frac{2\pi\mu\alpha k^2}{G\rho_0(1+k^2)}J_1(\mu\alpha k)A_1\times(e^{\alpha kl}+e^{-\alpha kl})e^{-\alpha kd}\frac{J_0(\alpha kR)J_1(\alpha k\nu)}{\alpha k\nu},$$

where $\rho_D=\rho_0=2.7$ g/cm^3 for aluminum, $Y_D=$Young's modulus of the detector$=7\times10^{11}$ dyn/cm^2, $Q_D=$figure of merit of the detector$\simeq10^5$, $L=\frac{1}{2}$ length of the detector$\simeq l\simeq77$ cm, $\alpha_D\simeq\alpha\simeq0.02$ cm^{-1}, $\nu=30$ cm

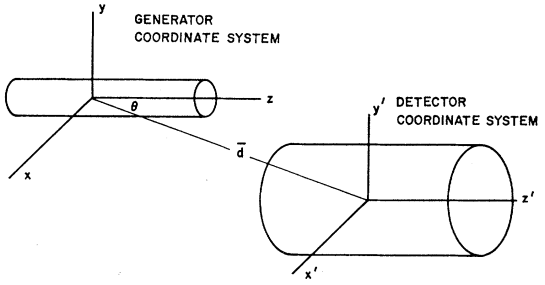

FIG. 2. Generator and detector coordinate systems.

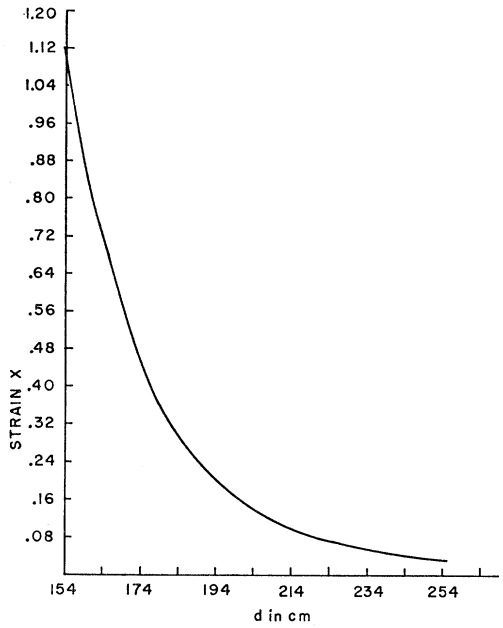

FIG. 3. Coaxial strain X in detector versus d, the distance between detector and generator centers for a strain of 0.5×10^{-4} in the generator. X is expressed as a multiple of $10^{-15}e^{i\omega t}\times\cos[(0.02\ \mathrm{cm}^{-1})z']$, where z' is defined in Fig. 2.

$=$radius of the detector, $k=$a dimensionless dummy variable, $\omega_D=\omega=10^4\ \mathrm{sec}^{-1}$ for this experiment, $\epsilon_{\mathrm{Dyn}}'(z',R,t)=$strain in the detector$=[d\xi_{\mathrm{Dyn}}'(z',R)/dz']e^{i\omega t}$, $d=\bar{d}\cos\theta$.

The equation for ϵ_{Dyn}' was calculated on the IBM 7090 computer and the curves of Figs. 3 and 4 were obtained.

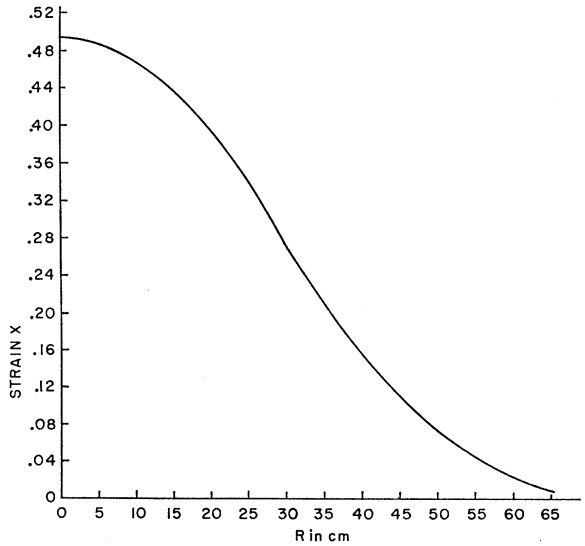

FIG. 4. Strain X in detector at $d=172$ cm versus R, transverse displacement of bars, for a strain of 0.5×10^{-4} in the generator. X is expressed as a multiple of $10^{-15}e^{i\omega t}\cos[(0.02\ \mathrm{cm}^{-1})z']$, where z' is defined in Fig. 2.

III. DEVELOPMENT AND DESCRIPTION OF THE APPARATUS

The natural resonant frequency of the generator was measured to be 1659.45 cps at 70°F. The detector has a natural resonance of 1657.52 cps at the same temperature. The resonant frequency of these rods varies inversely as their temperature. Because the generator mass is roughly $\frac{1}{10}$ that of the detector, the generator is the logical choice to be temperature controlled in order to match the resonant frequencies of the two rods.

The average strain in the generator during most of the experiment was 0.5×10^{-4} but it was taken as high as 10^{-4}. These values are well below the yield point of the bar. The generator is supported about its center by 3/32-in.-diam piano wire. It is stabilized longitudinally by a piano-wire clamp that presses against the top of the bar at the center. The support is an energy sink but, hopefully, the least lossy practical one.

Figure 5 is a block diagram of the generator. The piezoelectric transducers used to drive the generator are barium titanate with silvered surfaces that are provided with electrical leads. They are 2 in.$\times$2 in.$\times$0.2 in. and are molded to fit snugly to the bar. When an ac voltage is applied to the silvered surfaces of the transducers, an ac electric field exists perpendicular to the 2-in.-square surfaces. Because the transducers are piezoelectric, they oscillate along their length which is parallel to the bar axis. The vacuum in the generator chamber is maintained at diffusion pump pressures (less than 1 μ) in order to eliminate glow discharge resulting from the large ac voltages of 700 V rms applied to the transducer leads. Two driving transducers are employed in the experiment. They are bonded to the generator bar, near the center, and diametrically opposite one another in order to eliminate any motion of the bar in a bending mode. The frequency of the electrical signal on the transducers and hence of the excitation of transducers and bar is the frequency of the fundamental longitudinal resonant mode of the bar.

The limiting factor on the strains that are produced in the generator is the epoxy bond between the driving transducers and the bar. It is best to use a freely flowing epoxy because, when the transducer is pressed onto the bar, the possibility of air pockets getting trapped under the crystal is minimized. The best bond available at the time of the execution of the experiment was Eastman 910 with surface activator. It hardens in approximately 10 sec and withstands strains of $\simeq0.5\times10^{-4}$ at 1600 cps continuously for months.

Small quartz piezoelectric strain gauges are bonded to the generator near its center in order to monitor the strain.

The generator is operated in vacuum because of the large intensity acoustic noise it would make in air. The vacuum chamber is brass, cylindrically shaped, and contains high-pressure electrical fittings to connect to the drive and pickup transducers and the heating coil.

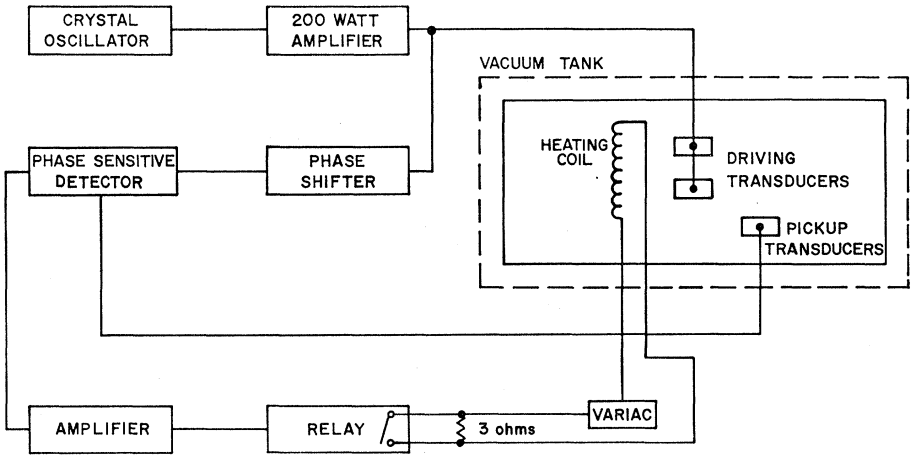

FIG. 5. Generator block diagram.

Because of the high Q of the detector, its response function is sharply peaked at its fundamental resonant frequency, the bandwidth being of the order of 0.01 cps. It would be a nearly impossible task to simply cut the generator to the exact length such that its fundamental resonance is within 0.01 cps of the detector and, even if the generator is cut to the precise length required, any slight change in room temperature would unbalance the equality of the resonant frequencies. It therefore becomes necessary to temperature control the generator automatically via a servo system and heating coil in order to ensure that the generator fundamental resonant frequency is always within the bandwidth of the detector resonant frequency. The experimentally determined coefficient of resonant frequency change as a function of temperature for the generator bar is $(1/f)df/dT = -272\times10^{-6}/°C$. A temperature bias is established by decreasing the generator's length such that it will always have to be heated well above room temperature in order for its resonant frequency to equal that of the detector. Then, by carefully controlling the current in a heating coil wrapped around the center of the generator, its temperature is cycled as slowly as possible about the temperature corresponding to the resonant frequency of the detector. The power dissipated in the generator due to its internal motion when it is driven at a strain of 0.5×10^{-4} at 1660 cps is 0.42 W. The continuously dissipated power raises the bar temperature 0.17°C, which is a negligible temperature increase compared to the temperature variations of the bar induced by the current in the heating coil. The heating coil, an ordinary 1000-W, 21-Ω element, is enclosed in ceramic washers which are, in turn, bonded to the bar with a cement that cures to a rubbery consistency and withstands high temperatures and large dynamic strains.

In order that the gravitational interaction between the generator and the detector can be measured, it is necessary that all other interactions be smaller. Other interactions that are eliminated are acoustic, electromagnetic, and vibrational. The detector responds to a kT of energy over its relaxation time of 30 sec. The driving power for the generator consists of at least 100 W of electromagnetic energy at the detector frequency. Extreme precautions are therefore required to avoid acoustic and electromagnetic leakage. Over 25 orders of power attenuation are, in fact, achieved.

The acoustic interaction between generator and detector is reduced primarily by mounting the bars in separate vacuum chambers. However, the entire generator vacuum system vibrates at the frequency of oscillation of the bar. This results from the radial vibration of the bar, which accompanies the longitudinal oscillations, being transmitted via the piano-wire support to the generator vacuum chamber. The vibration of the vacuum tank is decoupled from the floor of the lab by a filter stack consisting of alternate layers of felt, steel, and rubber. Alternating the density of the support material reflects the vibration at the interfaces between layers while heavy masses such as steel act as a momentum sink for the vibration. The detector is also suspended on a similar filter stack of rubber and steel in its vacuum chamber. The ringing of the generator vacuum chamber is still transmitted acoustically via the air to the detector system. In order to diminish the transmission, the entire generator vacuum chamber as well as the filter stack is enclosed in a plywood box lined with acoustic tile and filled with Dilite. More important, however, are the following improvements on the acoustic isolation of the detector: a concentric quartz coaxial transmission line between the bar and the matching electronics, a shielded rubber O ring to dampen vibration between the vacuum tank and the coax, and the enclosing of much of the detector electronics in anachoic boxes. Finally, a sonic shield of wood and acoustic tile is placed between the generator and the detector and the generator is placed in an 8-ft×8-ft ×12-ft room whose walls are lined with acoustic tile. These latter changes, particularly the improvements on the detector, reduce the acoustic interaction between the two systems to an acceptable level.

The acoustic sensitivity of the detector to a loudspeaker emitting noise of clearly audible intensity at its resonant frequency actually proved useful. By driving the loudspeaker with the crystal oscillator and slowly varying the frequency of the driving signal, the response peaks of the detector can be located. Since the detector consists of two closely coupled high-Q sections (the bar and the tuned LC circuit), there are two large-amplitude peaks at slightly different frequencies in the detector response characteristics. The gravitational interaction can be detected driving the generator at either frequency. The amplitude of the response at both peaks is identical if the detector is exactly tuned. The beat period between the two modes of oscillation is 18.50 sec. The loudspeaker actually excites the LC-circuit section of the detector whereas the dynamic gravitational field excites the bar section of the detector. As the LC-circuit section is detuned from the bar, one of the response peaks increases and the other decreases for excitation of the LC circuit.

The electromagnetic coupling problem involves coupling via radio frequency (rf) fields and coupling via the ground configuration of the generator and the detector. Elaborate shielding is invoked on the generator electronics including a steel chest to shield the amplifier and copper screening to shield the acoustic isolation room. The detector amplifiers are powered from batteries in order to isolate them from the line voltage and both the detector and generator systems are operated ungrounded.

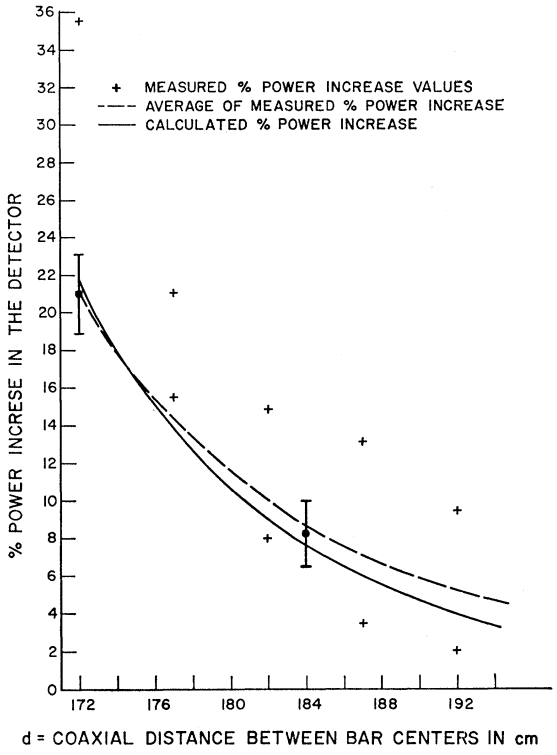

FIG. 6. % power increase in the detector versus distance between bar centers.

IV. RESULTS AND CONCLUSIONS

The raw data from the detector system are in mV. For each data point corresponding to a specific configuration of the generator and detector, two sets of voltages are taken and averaged. One set is taken with the generator frequency tuned to the detector frequency, and the other set corresponds to the generator frequency detuned from the detector frequency. The dynamic gravitational-field-induced strain in the detector is proportional to the square root of the differences of the squares of the average voltages. Runs at $d \geq 90$ in. showed no acoustic or electromagnetic leakage. A "run" consists of four data points corresponding to a detector and generator configuration; (1) coaxial and the distance between centers is 172 cm, (2) coaxial and the distance between centers is 184 cm, (3) 20 cm between axes and $d=172$ cm, and (4) 30 cm between axes and $d=172$ cm. Each data point requires 6 h of running time during which 360 voltage values (one per minute) are recorded from the detector. Ten runs were completed for the curves of Figs. 6 and 7. Some data points were taken at other than the above four configurations in order to check the general trend of the curves.

The circles on the curves of Figs. 6 and 7 represent the averages for the data points taken at a specific spatial configuration of the generator and detector. The error bars represent the standard deviation of the mean value of 10 runs and indicate the range of values in which there is a 68% chance that some new mean value of 10 additional runs would be included.

In order to calculate the proportionality constant between the voltages punched out on paper tape from the detector and the actual strain in the detector, a lengthy calculation involving the detector parameters must be done. It includes the characteristics of the bar, the sensing crystals, the LC circuit, the preamplifier and the amplifier. This calculation was done by J. Weber and will be published separately. The result of Weber's calculation is to determine the actual induced power increase in the detector when the bars are coaxial and 172 cm center-to-center and the strain in the generator is 0.5×10^{-4}. The induced power increase is proportional to the square of the induced strain.

Weber measured the system temperature of the detector and obtained 267.0°K±5% for the condition of no induced signal in the detector. He further calculated that the mean increase in temperature expected due to a strain in the generator of 0.5×10^{-4} and the detector and generator 172 cm apart center-to-center is 58.0°K. This represents a calculated power increase of 21.7%. From this value it is possible to plot the theoretically expected % power increase versus bar configurations

using the formula

$$[\text{Calculated \% power increase at } (d,R)=(i,j)]$$
$$=[\text{\% power increase at } (d,R)=(172,0)]$$
$$\times\left(\frac{\epsilon_{\text{theoretical}} \text{ at } (d,R)=(172,0)}{\epsilon_{\text{theoretical}} \text{ at } (d,R)=(i,j)}\right)^{-2}.$$

Here $[\epsilon_{\text{theoretical}}$ at $(d,R)=(172,0)]/[\epsilon_{\text{theoretical}}$ at $(d,R)=(i,j)]$ is obtained from Figs. 3 and 4. This plot is shown in Figs. 6 and 7 by a solid line. The measured % power increase curve is drawn as a dashed line. The

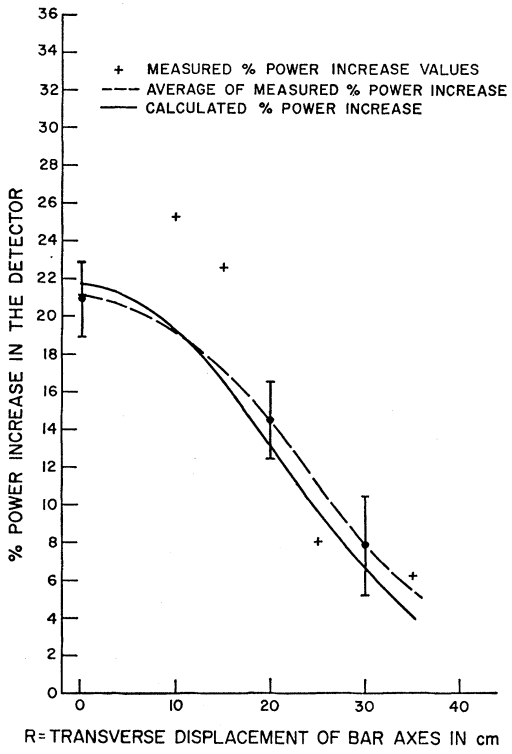

FIG. 7. % power increase in the detector versus transverse displacement of bar axes.

TABLE I. Comparison of measured and calculated power increases.

d, R (cm)	Average measured % power increase	Calculated % power increase	% deviation
172, 0	(21.0±2.1)	(21.7±2.0)	−0.7
184, 0	(8.3±1.7)	(7.6±0.7)	+0.7
172, 20	(14.5±2.1)	(13.2±1.2)	+1.3
172, 30	(7.9±2.6)	(6.5±0.6)	+1.4

experimental values averaged over the 10 runs compare very favorably with theory as seen in Table I.

The above comparison between measured % power-increase values and calculated % power-increase values shows that the calculated % power increase decreases slightly faster with distance than the measured % power increase. One explanation for this result is that there could be a small amount of leakage between generator and detector of a nongravitational nature. If the leakage is approximately equal in absolute magnitude for all runs, it will produce a bigger error in % power increase for the small-signal runs than for the large-signal runs.

V. SUMMARY

The gravitational induction field communications experiment described in this paper represents the first laboratory-achieved generation and detection of dynamic Newtonian fields in the kilocycle frequency range. Although the theory of this experiment is well known, its execution in the laboratory is extremely difficult. The experiment also fulfills its primary motivation, which is to calibrate a detector of gravitational radiation. The laboratory results conform very closely to theoretical predictions.

ACKNOWLEDGMENTS

The author is deeply indebted to Professor J. Weber for his invaluable help and guidance throughout a long and arduous search. Further acknowledgment is due Professor D. Zipoy, R. Clemens, and D. Gretz for their assistance during various tages of the experiment.